JACS
JOURNAL OF THE AMERICAN CHEMICAL SOCIETY
pubs.acs.org/JACS
Article

# Soft Mode Metal-Linker Dynamics in Carboxylate MOFs Evidenced by Variable-Temperature Infrared Spectroscopy

Anastasia B. Andreeva, Khoa N. Le, Lihaokun Chen, Michael E. Kellman, Christopher H. Hendon,* and Carl K. Brozek*

Cite This: J. Am. Chem. Soc. 2020, 142, 19291−19299
Read Online
ACCESS | Metrics & More | Article Recommendations | Supporting Information

**ABSTRACT:** Through comprehensive analysis of carboxylate-based metal−organic frameworks (MOFs), we present general evidence that challenges the common perception of MOF metal-linker bonds being static. Structural dynamics in MOFs, however, typically refers to the "breathing" behavior of cavities, where pores open and close in response to guest molecules, and to the transient binding of guest molecules, but dynamic bonding would explain important MOF phenomena in catalysis, postsynthetic exchange, negative thermal expansion, and crystal growth. Here, we demonstrate, through use of variable-temperature diffuse reflectance infrared Fourier transform spectroscopy (VT-DRIFTS) aided by ab initio plane wave density functional theory, that similar evidence for melting behavior in zeolitic imidazolate frameworks (ZIFs), i.e., reversible metal-linker bonding, driven by specific vibrational modes, can be observed for carboxylate MOFs by monitoring the red-shifts of carboxylate stretches coupled to anharmonic metal-carboxylate oscillators. To demonstrate the generality of these findings, we investigate a wide class of carboxylate MOFs that includes iconic examples with diverse structures and metal-linker chemistry. As the very vibrations invoked in ZIF melting but heretofore unobserved for carboxylate MOFs, these metal-linker dynamics resemble the ubiquitous soft modes that trigger important phase transitions in diverse classes of materials while offering a fundamentally new perspective for the design of next-generation metal−organic materials.

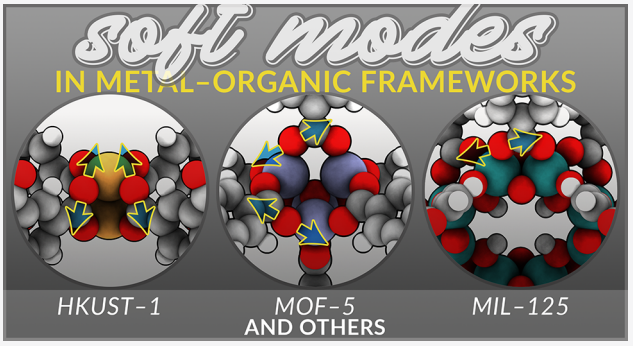


## INTRODUCTION

Important material phenomena often depend on dynamic distortions to solid lattices, such as ion diffusion through solid electrolytes[1] and surface reconstruction of heterogeneous catalysts.[2] In particular, certain lattice vibrations cause such extreme distortions to equilibrium geometries that they trigger structural phase transitions responsible for wide-ranging functional properties,[3] including ferroelectricity,[4−7] metal−insulator transitions,[8] exciton condensation,[9,10] and multiferroics.[11] Monitoring these phonon modes as a function of temperature reveals that the peak positions redshift and intensities diminish near the phase change critical temperature due to the vibrations transferring energy into the structural reordering process through anharmonic coupling to other phonons.[12] Because these vibrations dissipate energy, they are termed "soft modes". Analysis of such vibrations, and their coupling to magnetic, vibrational, electronic, and other degrees of freedom, offers a microscopic basis for predicting and controlling phase transitions.[13] Understanding the relationship of lattice dynamics to phase transitions has guided the design of new types of materials, such as metastable phases, for devices with specifically enhanced physical properties. Recently, metal-linker dynamics in the porous coordination polymers known as metal−organic frameworks (MOFs) have been invoked to describe melting mechanisms of MOF liquids[14−18] and glasses.[19−26] These disordered MOF materials attract considerable attention by opening possibilities in the design of porous materials for applications ranging from gas storage to ion exchange membranes, but the metal−ligand dynamics associated with their melting transitions challenge the common conception of MOFs as static structures. Although metal-linker lability helps explain melting and other important behavior, evidence for such dynamic coordination chemistry has only been observed indirectly for carboxylate MOFs.[27−29] Direct measurement of metal-linker lability has been possible for certain ZIFs, however, requiring specialized high-temperature synchrotron techniques.[14,24] The intensifying research into dynamic metal−organic materials would benefit, therefore, from routine methods that probe metal-linker

Received: September 3, 2020
Published: October 29, 2020







https://dx.doi.org/10.1021/jacs.0c09499
J. Am. Chem. Soc. 2020, 142, 19291−19299

lability, especially for carboxylate MOFs, which constitute the overwhelming majority of MOFs.

Although reversible metal-linker coordination is thought to drive MOF crystallization, such dynamic bonding is not commonly thought to occur once the MOF is formed. Dynamic metal-linker bonding is well-documented in analogous one-dimensional coordination polymers, which comprise an important subset of materials termed "dynamic", "adaptable", "stimuli-responsive", or "self-healing covalent networks".[30−34] For example, formation constants (log $K_f$, $K_f$ = [bound metal linkers]/[unbound metal linkers]) of metal-pyridyl[35] and metal-carbene[36] polymers have been measured to be as small as 3 to 4, implying that "unbound" states constitute a significant portion of the polymer linkages.

Interestingly, formation constants of molecular metal-carboxylate complexes akin to MOF coordination moieties, e.g., zinc-benzoate, range from only 0.1 to 1.5.[37] Structural dynamics in MOFs, instead, conventionally refers to the pressure-induced "breathing" behavior of pore cavities,[38−41] the transient binding of guest molecules,[27,42−46] and the negative thermal expansion (NTE) of certain MOFs,[47−53] but labile metal-linker bonding would explain important phenomena, such as the ability of MOFs to undergo postsynthetic exchange,[54−60] perform catalysis at seemingly saturated metal centers,[61] and readily grow as bulk crystals. Reversible metal-linker bonding could also complement the current mechanistic understanding that dynamic linker motion drives NTE, and, more broadly, guide deliberate control over important MOF functions, while inspiring the design of porous materials with stimuli-responsive, metastable, self-healing, and other adaptable behavior. With challenging the common conception of carboxylate MOFs as static structures, evidence for their labile metal-linker bonding will enable their design in applications that leverage structural dynamics.

Here, we demonstrate variable-temperature diffuse reflectance infrared Fourier transform spectroscopy (VT-DRIFTS) as a convenient method for probing MOF metal-linker dynamics. We observe that at higher temperatures, carboxylate stretches red-shift for a general collection of representative carboxylate-based MOF materials, which we ascribe to thermal population of MOF conformations with "loose" metal-carboxylate linkages in equilibrium with a decreased population of "tight" metal-linker states. Importantly, the C−O stretches provide a convenient spectroscopic handle for metal-linker bonding dynamics, due to the coupling of the readily observable C−O modes to the more elusive M−O modes (Scheme 1A). A similar approach has been employed previously, where analysis of linker, rather than metal-linker vibrational modes, provided evidence for dynamic bonding in self-healing metal-pyridyl one-dimensional coordination polymers.[62] Variable-temperature Raman spectroscopy evidenced red-shifting pyridyl stretches at higher temperatures that were attributed to dynamic structural rearrangements.[62] Evidence for the melting mechanism of ZIFs rests on analysis of red-shifting zinc-imidazolate bond stretches, requiring specialized variable-temperature terahertz (THz)/Far-IR synchrotron techniques, due to the low-energy spectral range.[24] In these reports, consistent with analysis of other dynamic and phase-change systems, the red-shifting behavior was attributed to thermal population of the unevenly spaced vibrational excited states of an anharmonic Zn-imidazolate oscillator.[63] Because the states become more closely spaced at higher energies, the apparent vibrational mode shifts to lower wavenumbers. With

**Scheme 1. Molecular Orbital (MO) Description of MOF Metal-Carboxylate Interactions**[a]

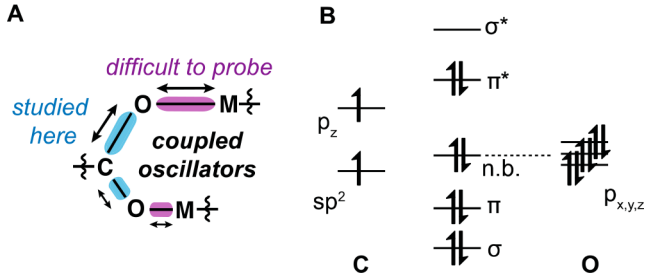


[a](A) Schematic representation of C−O and M−O coupled anharmonic oscillators in metal-carboxylate complexes. (B) MO diagram of carbonyl bond in a carboxylate group.

greater population of higher energy states, the vibrational amplitudes also increase until they reach a critical ratio with respect to the interatomic metal−ligand spacing, termed the Lindemann ratio,[64] causing the material to melt. Fundamentally, this behavior resembles the ability of soft modes to induce phase transitions through vibrational motion. Here, we demonstrate that similar evidence for melting behavior can be observed for carboxylate MOFs by monitoring the red-shifts of carboxylate stretches coupled to anharmonic metal-linker oscillators. We justify this strategy in terms of molecular orbital arguments and a simple two-state model of tight and loose metal-linker states in thermal equilibrium. The temperature-induced metal-linker dynamics evidenced in these prototypical MOFs resembles VT-DRIFTS studies of soft modes and phase changes in other classes of materials, including ZIFs, but had not been previously observed for ubiquitous carboxylate MOFs. Evidence for soft modes in carboxylate MOFs have been previously impeded by the difficulty of monitoring low-energy metal-linker vibrations directly, whereas the carboxylate stretches studied here provide a convenient alternative spectroscopic handle. To demonstrate the generality of these findings, we investigate a wide class of carboxylate MOFs that includes iconic examples with diverse structures and metal-linker chemistry. The broad applicability of these results offers a fundamentally different perception of MOFs. In addition to MOFs, we expect VT-DRIFTS to offer a powerful method for probing the stability, dynamics, and structure of other organic−inorganic materials featuring metal−ligand bonds, such as 1-D coordination polymers, porous liquids, and metal−organic cages.[65−67]

## RESULTS AND DISCUSSION

Molecular orbital (MO) theory provides a straightforward explanation for why carboxylate stretches might redshift with weaker metal-linker interactions. Scheme 1B illustrates a simplified MO diagram for an individual C−O bond of a carboxylate group. Because the highest energy electrons reside in orbitals that are anti/nonbonding with respect to the C−O bond, they act as the lone pair involved in dative interactions with metal ions. Accordingly, stronger M−O interactions would also enhance C−O bonding by distributing the antibonding density away from the C−O bond vector. Therefore, strong M−O interactions should cause blueshifts to carboxylate stretches, and weak M−O interactions should cause redshifts. Indeed, strongly ionic carboxylate complexes, such as sodium benzoate, show the highest-energy carboxylate


https://dx.doi.org/10.1021/jacs.0c09499
J. Am. Chem. Soc. 2020, 142, 19291−19299

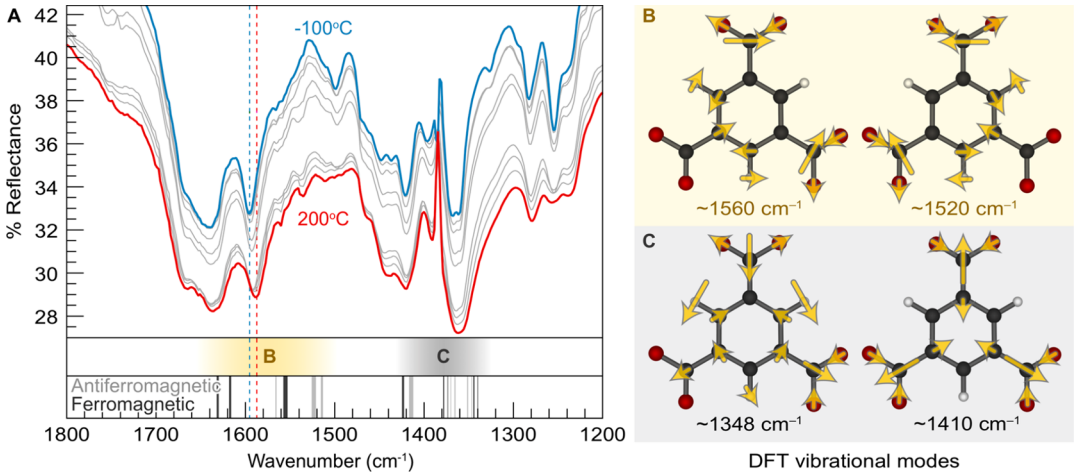


**Figure 1.** Variable-temperature diffuse reflectance infrared Fourier transform spectra (VT-DRIFTS) and computed phonon modes of HKUST-1. (A) (Top) Experimental spectra collected between −100 and 200 °C under dynamic vacuum. (Bottom) Simulated peak positions of phonon modes with carboxylate character denoted by color intensity and labeled according to modes shown in panel B. (B) Representation of "asymmetric" and (C) "symmetric" carboxylate-based phonon modes projected at the Γ q-point.

stretching modes. For similar reasons, interactions between Lewis acidic metal ions and carbon monoxide induce blueshifts to C−O stretching frequencies. Hence, we hypothesize that if MOF metal-linker bonds exist in equilibrium between "tight" and "loose" states, then high temperatures would produce redshifts by shifting the equilibrium toward weaker C−O interactions. Second, if observed carboxylate bands arise from overlapping spectral components from tight and loose species, then we expect band widths to maximize at temperatures where these species exist in equal mixtures and minimize at temperatures dominated by a single species.

The material HKUST-1 ($Cu_3$(1,3,5-benzenetricarboxylate)$_2$) was chosen as an initial target for VT-DRIFTS as many seminal studies of MOFs were first demonstrated with this material. Figure 1A plots the spectra collected at 50 °C intervals starting from room temperature, then warmed to 200 °C, and then cooled to −100 °C. Surprisingly, several bands, in addition to the expected asymmetric and symmetric carboxylate stretches, appear to redshift with increased temperature. Therefore, we employed density functional perturbation theory for proper assignment of all bands in Figure 1A. For emphasis, only bands with carboxylate character are plotted in Figure 1A, but full calculated spectra are included in the Supporting Information. As the Cu paddlewheel dimer in HKUST-1 displays antiferromagnetic ordering below 280 K,[68] which is within the measured temperature regime, spectra were simulated with both antiferromagnetic (AFM) and ferromagnetic (FM) ordering, with the former showing excellent agreement with spectra collected below room temperature (Figure 1A, bottom). To aid in band assignment, vibrational normal modes were projected at the Γ *q*-point and represented as molecular diagrams (Figure 1B), with arrows denoting vibrational directions and oscillator intensities. Interestingly, all contain carboxylate character, suggesting that the temperature dependence of the data in Figure 1A arises from orbital interactions involving carboxylates specifically. Among these bands, the symmetric carboxylate stretch shows the most distinctive redshift. Notably, the band unique to the AFM magnetic state helps account for the experimental feature, such as the peak at 1499 $cm^{-1}$, that disappears above 300 K. We therefore attribute this band to the calculated phonon at 1520 $cm^{-1}$. Consequently, we explicate the following analysis by focusing on this band in particular, although the symmetric and asymmetric carboxylate stretches of all MOFs considered here exhibit redshifts.

To highlight the apparent temperature dependence, Figure 2A plots the baseline-subtracted asymmetric carboxylate stretches collected between −100 and 200 °C. This band shifts by 5.8 $cm^{-1}$ from a maximum frequency of 1594.8 $cm^{-1}$ at −100 °C to a minimum value of 1589.0 $cm^{-1}$ at 200 °C. For closer inspection, Figure 2B shows the peak maxima versus temperature, cycled three times between −100 and 200 °C, with values obtained from Gaussian fits to each band. These data reveal a linear relationship between −100 and 200 °C with a slope, $X_a$, of −0.023 $cm^{-1}$/K and confirm reversibility, as expected for a process in thermodynamic equilibrium. Furthermore, the symmetric stretch shifts between 1367.9 and 1362.1 $cm^{-1}$ in this temperature regime (Figures S6, S7), while the additional peaks around 1640 and 1400 $cm^{-1}$ with partial carboxylate character also redshift. Interestingly, these plots resemble temperature-dependent vibrational studies of minerals, ZIFs, and other classes of materials that relate shifting peak maxima to interrelated concepts of phase changes, lattice instability, and structural dynamics. For example, the $\nu_2$ band of calcite, said to possess a "softer interatomic potential" than the other bands, exhibits a $X$ of −0.0049 $cm^{-1}$/K near the critical temperature for phase transitions into calcium carbonate polymorphs.[69] Redshifting vibrations have also been observed widely in other minerals, such as apatite, and are attributed to temperature-dependent anharmonic coupling between phonon modes.[70] Additionally, the zinc-imidazolate-based ZIF-UC-4 displays a $X$ of −0.00292 $cm^{-1}$/K in the crystalline phase and $X$ values of −0.00597 and −0.1377 $cm^{-1}$/K in the glass and liquid phases, respectively.[24] Taken together, these reports suggest that $X$ offers a measure of the susceptibility of bonds to distort in response to temperature. Larger slopes, therefore, represent weaker bonding. Importantly, the average full-width-at-half-maximum (fwhm) values increase from −100 °C to a maximum around 50 °C, followed by decreasing bandwidth toward 200 °C (Figure 2C). These data strongly suggest the presence of multiple spectral


https://dx.doi.org/10.1021/jacs.0c09499
J. Am. Chem. Soc. 2020, 142, 19291−19299

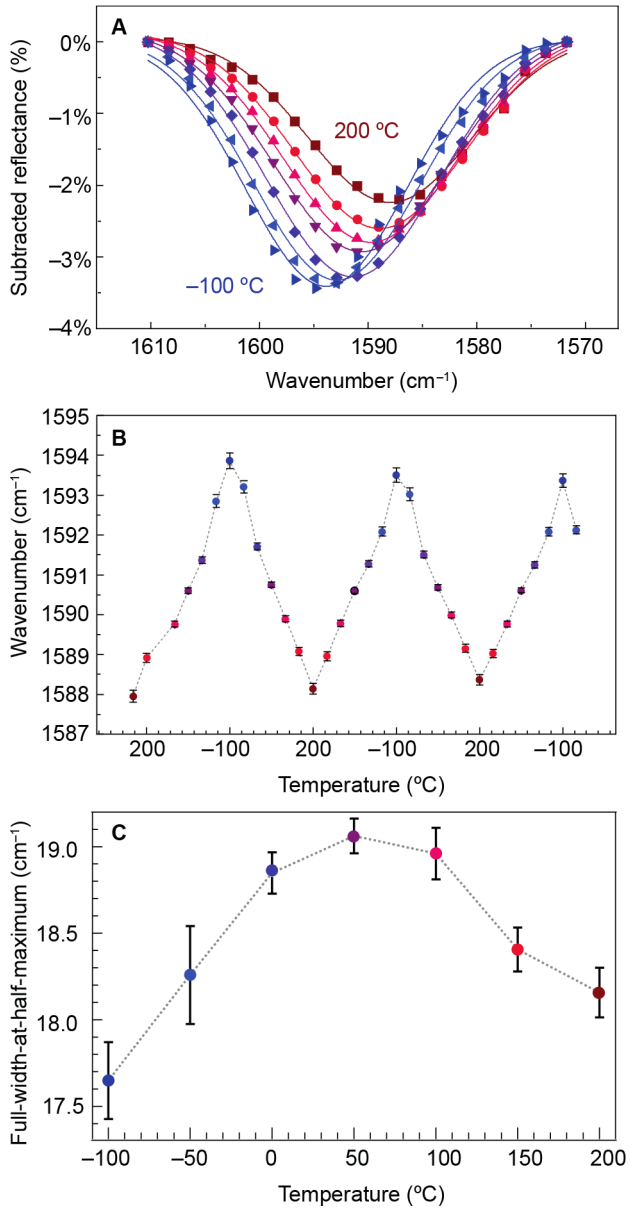


**Figure 2.** Temperature-dependent spectral data for the HKUST-1 asymmetric carboxylate vibrational mode. (A) Baseline-subtracted reflectance spectra, with experimental data shown as markers and Gaussian fits shown as solid lines. (B) Peak positions plotted against temperature across three continuous temperature ramp cycles, with error bars derived from Gaussian fits and data point colors corresponding to temperatures shown in panel A. (C) Full-width-at-half-maximum (fwhm) values averaged over three temperature ramp cycles. Error bars denote standard deviations from the averaged data.

components representing species in thermodynamic equilibrium.

To explore the generality of temperature-dependent MOF carboxylate stretches, a suite of representative MOF materials was investigated that offers a range of metal-carboxylate binding geometries and metal-linker bond strengths. These were chosen because seminal findings have been made with them as examples: Mg-MOF-74 ($Mg_2$(2,5-dihydroxyterephthalate)), Zn-MOF-74 ($Zn_2$(2,5-dihydroxyterephthalate)), MOF-5 ($Zn_4O$(1,4-benzenedicarboxylate)$_3$), MIL-125 ($Ti_8O_8(OH)_4$(1,4-benzenedicarboxylate)$_6$), MIL-125-$NH_2$ ($Ti_8O_8(OH)_4$(2-aminoterephthalate)$_6$), UiO-66 ($Zr_6O_6$(1,4-benzenedicarboxylate)$_6$), MUV-10(Ca) ($Ti_3Ca_3O_2$(1,3,5-benzenetricarboxylate)$_4$), and MUV-10(Mn) ($Ti_3Mn_3O_2$(1,3,5-benzenetricarboxylate)$_4$). All materials were subjected to identical measurement conditions, and resulting spectra were analyzed by comparing to simulated spectra, as described for HKUST-1. Indeed, all MOFs exhibited clear red-shifts to vibrational modes upon being heated from −100 to 200 °C, as summarized in Table 1. As expected for a diverse collection of

**Table 1. Summary of Asymmetric ($X_a$) and Symmetric ($X_s$) Red-Shift Slopes of Carboxylate Materials Studied Here through VT-DRIFTS Collected under Dynamic Vacuum**

| MOF Name | $X_a$ (cm$^{-1}$/K) | $X_s$ (cm$^{-1}$/K) |
|---|---|---|
| HKUST-1 | −0.021 | −0.020 |
| MUV-10 (Ca) | −0.019 | −0.019 |
| MUV-10 (Mn) | −0.015 | −0.041 |
| Mg-MOF-74 | −0.027 | −0.0087 |
| Zn-MOF-74 | −0.023 | −0.0042 |
| MOF-5 | −0.026 | −0.0095 |
| MIL-125 | −0.0093 | −0.019 |
| MIL-125-$NH_2$ | −0.036 | −0.066 |
| UiO-66 | −0.015 | −0.020 |
| Sodium benzoate | −0.015 | −0.024 |

coordination environments and orbital interactions, the observed temperature-induced shifts vary significantly between MOF materials, even between isostructural analogs. Interestingly, the asymmetric stretch, typically ascribed to the C=O double bond character, exhibited greater sensitivity in certain materials, such as MOF-5, Mg-MOF-74, and Zn-MOF-74, whereas the symmetric stretch, often associated with C−O single bond character, showed greater sensitivity in others. On the basis of this interpretation, symmetric and asymmetric frequencies should be similar for carboxylates with greater resonance bond character, and hence more uniform electron delocalization. Accordingly, MOFs with asymmetric ligands, MIL-125-$NH_2$ and MOF-74, exhibited the biggest differences between $X_a$ and $X_s$. According to the MO explanation, the linker-based stretching frequencies of MOFs with strong metal-linker bonds should show little if any temperature dependence. This interpretation helps explain the temperature-independent triazolate stretches observed in VT-DRIFTS studies of Zn-CFA-1.[71] Interestingly, MIL-125, MIL-125-$NH_2$, and UiO-66, show temperature-dependent carboxylate shifts despite their notable structural stabilities. Yet, as expected, the observed redshifts slopes $X$ appear smallest among these examples. Because molecular metal carboxylate complexes feature similar orbital interactions to these MOFs, they should also exhibit such temperature dependence. Indeed, we observe from VT-DRIFTS measurements that sodium benzoate shows large shifts to both asymmetric and symmetric carboxylate stretches (Table 1). Comparison between isostructural MOFs also offers insight into differences in bonding interactions. The large redshift slopes observed for Mg-MOF-74, for instance, may be attributed to the lower electronegativity of Mg relative to Zn, giving rise to weaker metal-carboxylate bonding.

Rather than reproduce the observed redshifts from empirical parameters, we investigated whether the experimental data could be simply fitted to two equilibrium species in relative ratios appropriate for labile metal-carboxylate bonds. Indeed, a global population analysis of the symmetric carboxylate stretch for HKUST-1 indicates that the temperature-dependent band


https://dx.doi.org/10.1021/jacs.0c09499
J. Am. Chem. Soc. 2020, 142, 19291−19299

can be accurately deconvoluted into a higher-energy component at 1596 $cm^{-1}$ that decreases in intensity and a lower-energy component at 1587 $cm^{-1}$ that increases in intensity with increased temperature (Figure 3). Importantly,

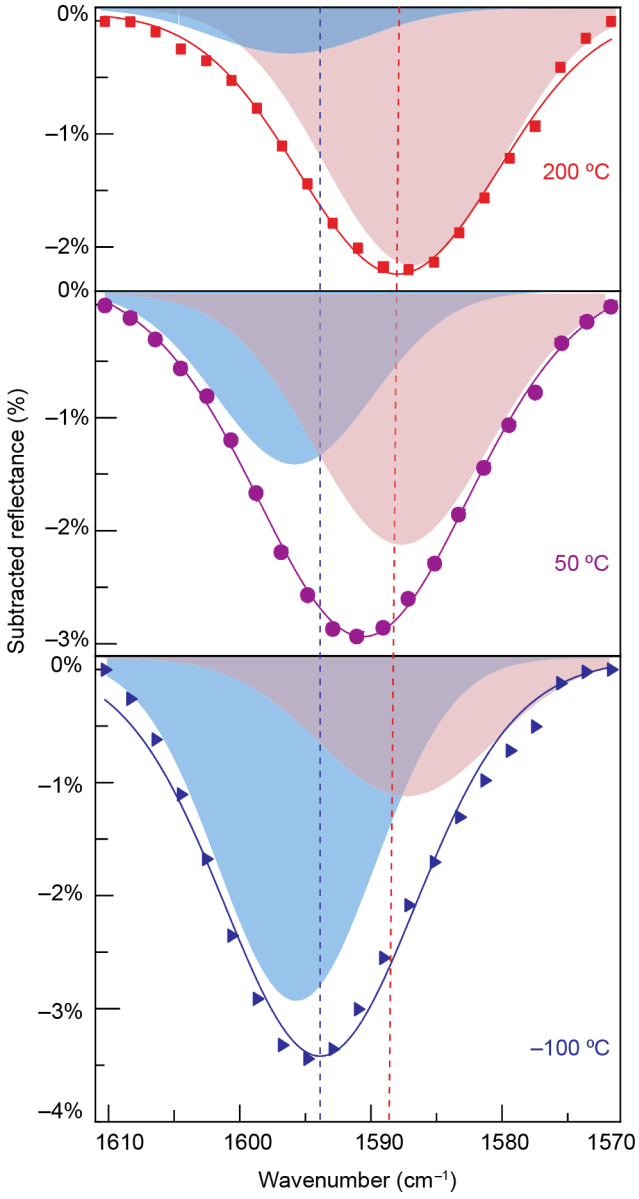


**Figure 3.** Global curve fittings for representative spectra of the HKUST-1 asymmetric carboxylate stretch. Spectral deconvolution assumed two components with constant peak maxima but variable total areas. Fits produced a species centered at 1596 $cm^{-1}$ (blue) and another at 1587 $cm^{-1}$ (red). Markers denote experimental data and solid lines show Gaussian fits. Global curve fitting was performed for all data shown in Figure 2.

the frequencies of these two components remain unchanged during the data fitting, as expected for a two-state model. Furthermore, this analysis corroborates the evidence in Figure 2C for a dominant species existing at either temperature extreme but with nearly equal populations around 50 °C. Scheme 2 illustrates this chemical scenario where each component represents ensembles of metal carboxylate species with either long "loose" or short "tight" interactions, each integrated across shallow potential energy surfaces.

**Scheme 2. Equilibrium between "Tight" and "Loose" Ensembles of MOF Metal-Carboxylate Populations Existing near Thermoneutral Equilibrium**[a]

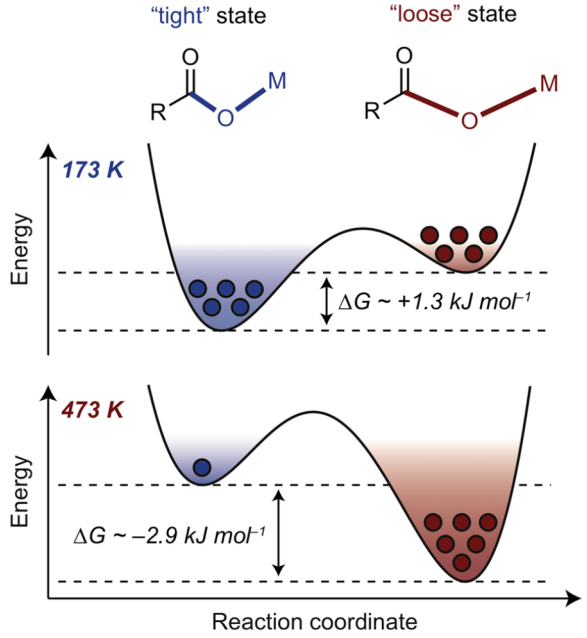


[a](Top) Conversion of MOF metal-linker bonds between two ensemble-averaged states. (Bottom) Temperature-dependent free energies ($\Delta G$) and relative population according to equilibrium constants derived from experimental data.

To examine whether this spectral deconvolution supports the existence of dynamic metal-carboxylate bonds, we determined stability constants from the integrated relative ratios of both components at each temperature. As $K_f$ relates bound-to-unbound ratios by convention, Figure 4 instead shows plots of $K$ ([loose]/[tight]) versus temperature for convenience because the lower-energy 1587 $cm^{-1}$ feature associated with the loose state emerges with increased temperature. Importantly, the room temperature log $K$ value

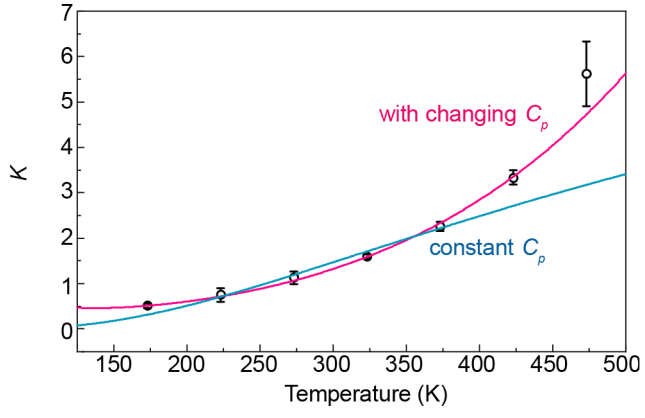


**Figure 4.** van't Hoff analysis of MOF metal-linker dynamic equilibrium. Inverse stability constants K ([loose]/[tight]) were determined as the ratio of integrated spectral components determined by global curve fitting of the HKUST-1 asymmetric stretch. Data points represent average values from three temperature ramp cycles, with error bars denoting standard deviations. Data were fit to a standard van't Hoff equation assuming constant material specific heat (blue) and an equation with changing specific heat (pink).



https://dx.doi.org/10.1021/jacs.0c09499
J. Am. Chem. Soc. 2020, 142, 19291−19299

of ∼0.6 corresponds well to the reported values of molecular metal-carboxylate complexes, which range from ∼0.1 to 1.5 for common MOF metal ions.[37] Such small $K$ values imply a surprising degree of MOF metal-linker lability, in sharp contrast with the common conception of MOFs as being static entities.

For further thermodynamic insight into the MOF metal-linker equilibrium, we performed van't Hoff analyses of $K$ versus temperature data. Figure 4 includes fits from a conventional analysis ($K = \exp[-(\Delta H - T\Delta S/RT)]$) and another ($K = \exp[-(\Delta H + \Delta C_P(T - 298.15\ \mathrm{K}) - T(\Delta S + \Delta C_P \ln(T/298.15\ \mathrm{K})))/RT)]$) that accounts for a changing material specific heat ($\Delta C_P$), as was applied previously to equilibrium mixtures of dynamic structures,[72] such as H-bonding networks and phase change materials. Interestingly, accounting for $\Delta C_P$ afforded a far superior fit to the data, lending further support for the red-shifting carboxylate stretches being indicators of lattice dynamical motion. This fitting procedure afforded values of $\Delta H = 5.9 \pm 0.2$ kJ mol$^{-1}$, $\Delta S = 22.0 \pm 0.6$ J mol$^{-1}$ K$^{-1}$, and $\Delta C_P = 37 \pm 4$ J mol$^{-1}$ K$^{-1}$ suggesting that this process involves a slight endothermic barrier overcome by increases in entropy, as expected for a thermally activated bond disruption process near equilibrium. A changing specific heat further supports the explanation that the red-shifting spectra arise from soft mode behavior, as material specific heats become infinite near the critical temperatures of phase changes.

Through advanced analytical techniques, recent investigations have made considerable progress in characterizing MOF structural disorder and dynamics,[14,27,73,74] but experimental evidence for the precise geometries of dynamic systems remains an outstanding challenge. For example, variable temperature X-ray diffraction data of HKUST-1 reveal negative thermal expansion, superficially suggesting bond contraction, rather than expansion, at higher temperatures. After careful consideration, these results can be attributed to large, "trampoline-like" dynamic distortions of the linkers at high temperatures that become time-averaged into a static crystallographic structure disguising the true elongated distances.[47] Nevertheless, evidence for metal-linker dynamics is apparent in the highly disordered carboxylate oxygens, which create the greatest thermal displacements. For structural insight into the tight and loose configurations of HKUST-1, we therefore computed geometries across a range of contracted and expanded unit cell volumes. Figure S45 plots the total energies of structures resulting from lattice distortions that correspond to temperatures spanning ±444 K based on reported thermal expansion coefficients.[47] These simulated data contain several important features that support our model: the shallow depth of the energy well is consistent with numerous, degenerate metal-carboxylate structures; the existence of multiple energetic minima resemble the tight and loose species in thermal equilibrium (highlighted in red and blue as potential candidates); and the direct relationship between Cu−O and C−O distances supports our claim that monitoring carboxylate stretches serves as a proxy for studying MOF metal-carboxylate dynamics. As expected for coupled anharmonic oscillators, this imbalanced relationship causes the Cu−O bond to be much more sensitive than the C−O carboxylate fragment: over the explored temperature range, the Cu−O bond shows a 20-fold greater slope that covers a considerable bond difference of nearly 0.01 Å compared to just 0.0006 Å for C−O. These results emphasize the remarkable ability of VT-DRIFTS to produce spectral features of such small carboxylate distortions as evidence for major distortions to metal-carboxylate bonds studied only with great difficulty.

Redshifting MOF carboxylate stretches resemble lattice dynamical soft modes observed at temperatures near the phase transition critical temperatures ($T_c$) for numerous materials, such as ferroelectric perovskites and ZIFs.[5,6,75,76] Although described by different physical models, both involve large-amplitude vibrations that drive structural phase changes. According to soft mode theory, the frequency of these critical vibrations redshifts and then vanishes as the material assumes a new structure with unique normal modes. In the data presented here, we attribute the redshift of the carboxylate modes to the gradual transition of a crystalline form into an amorphous structure with weaker metal-carboxylate bonds and a new corresponding set of normal modes. Interestingly, these data resemble the spectral evidence of melting behavior in ZIFs, and yet melting has yet to be observed in carboxylate MOFs. Computational simulations suggest, however, that metal-carboxylate soft modes drive breathing behavior in MOFs,[77] although direct evidence remains an outstanding challenge. These data, therefore, suggest that carboxylate-based MOFs undergo structural distortions associated with melting transitions but decompose before reaching the melting point. A key difference that may explain the absence of melting carboxylate MOFs is that while ZIFs include individual metal ions, carboxylate MOFs often contain multimetallic metal nodes. Upon dissociation from linkers, these complex inorganic fragments may recombine with nearby dangling linker molecules into any numerous possible polymorphs and amorphous decomposition products rather than remain in a melted phase resembling the original crystalline lattice. Therefore, these results suggest that melting may be achievable in carboxylate MOFs with few competing polymorph phases, perhaps such as those with mononuclear metal sites. While offering evidence for the existence of soft modes invoked to describe MOF liquids, these data provide mechanistic justification of other MOF phenomena requiring dissociation of MOF metal-linker bonds: most notably, single-crystal-to-single-crystal postsynthetic modification (cation exchange and ligand exchange),[54,59,60,78] the ability of MOFs to encapsulate molecules larger than their pore apertures,[79] and the negative thermal expansion of MOFs.[47−50,52,53,80,81] Identification and analysis of soft modes in phase change MOFs also offers a tool for investigating fundamental aspects of how molecular structure drives phenomena spanning spin crossover transitions, symmetry-lowering distortions, and ferroelectricity.

## CONCLUSION

VT-DRIFTS provides strong evidence for dynamic metal-linker bonding in carboxylate-based MOFs. Redshifts to carboxylate vibrational modes can be modeled accurately as equilibrium mixtures of tight and loose metal-linker species, producing $K$ values remarkably consistent with the well-documented lability of molecular analogs. Additionally, carboxylate stretches serve as convenient spectroscopic alternatives to metal-linker vibrational modes for studying structural dynamics that have eluded recent investigations into liquid MOFs and MOF glasses. Taken together, this previously unobserved evidence for MOF metal-linker dynamics builds on recent evidence that challenges the fundamental perception of MOFs as static structures, offering mechanistic justification for important MOF phenomena and a powerful tool for leveraging


https://dx.doi.org/10.1021/jacs.0c09499
J. Am. Chem. Soc. 2020, 142, 19291−19299

MOF structural dynamics in the design of next-generation adaptable materials.

## ■ ASSOCIATED CONTENT

### Supporting Information

The Supporting Information is available free of charge at https://pubs.acs.org/doi/10.1021/jacs.0c09499.

Syntheses, experimental details, supplementary figures and tables, additional VT-DRIFTS, and DFT data (PDF)

## ■ AUTHOR INFORMATION


### Corresponding Authors

**Carl K. Brozek** − *Department of Chemistry and Biochemistry, Materials Science Institute, University of Oregon, Eugene, Oregon 97403-1253, United States;* orcid.org/0000-0002-8014-7904; Email: cbrozek@uoregon.edu

**Christopher H. Hendon** − *Department of Chemistry and Biochemistry, Materials Science Institute, University of Oregon, Eugene, Oregon 97403-1253, United States;* orcid.org/0000-0002-7132-768X; Email: chendon@uoregon.edu

### Authors

**Anastasia B. Andreeva** − *Department of Chemistry and Biochemistry, Materials Science Institute, University of Oregon, Eugene, Oregon 97403-1253, United States*

**Khoa N. Le** − *Department of Chemistry and Biochemistry, Materials Science Institute, University of Oregon, Eugene, Oregon 97403-1253, United States*

**Lihaokun Chen** − *Department of Chemistry and Biochemistry, Materials Science Institute, University of Oregon, Eugene, Oregon 97403-1253, United States*

**Michael E. Kellman** − *Department of Chemistry and Biochemistry, Materials Science Institute, University of Oregon, Eugene, Oregon 97403-1253, United States;* orcid.org/0000-0002-6198-8812

Complete contact information is available at: https://pubs.acs.org/10.1021/jacs.0c09499


### Notes

The authors declare no competing financial interest.

## ■ ACKNOWLEDGMENTS

We gratefully acknowledge the University of Oregon for startup funds and thank C. E. Bein and Profs. S. W. Boettcher, C. R. Wade, and D. C. Johnson for insightful conversations. This work made use of the CAMCOR facility of the Lorry I. Lokey Laboratories at the University of Oregon to perform VT-DRIFTS experiments. This material is based upon work supported by the National Science Foundation through the Division of Materials Research under grant no. DMR-1956403. We also acknowledge the continued support from the Extreme Science and Engineering Discovery Environment (XSEDE), which is supported by the National Science Foundation [ACI-1548562] and the PICS Coeus High Performance Computer, which is supported by the National Science Foundation [1624776].

## ■ REFERENCES


(1) Famprikis, T.; Canepa, P.; Dawson, J. A.; Islam, M. S.; Masquelier, C. Fundamentals of Inorganic Solid-State Electrolytes for Batteries. *Nat. Mater.* **2019**, *18* (12), 1278−1291.

(2) Sachs, C.; Hildebrand, M.; Volkening, S.; Wintterlin, J.; Ertl, G. Spatiotemporal Self-Organization in a Surface Reaction: From the Atomic to the Mesoscopic Scale. *Science* **2001**, *293* (5535), 1635.

(3) Scott, J. F. Soft-Mode Spectroscopy: Experimental Studies of Structural Phase Transitions. *Rev. Mod. Phys.* **1974**, *46* (1), 83−128.

(4) Cochran, W. Crystal Stability and the Theory of Ferroelectricity. *Adv. Phys.* **1960**, *9* (36), 387−423.

(5) Dunnett, K.; Narayan, A.; Spaldin, N. A.; Balatsky, A. V. Strain and Ferroelectric Soft-Mode Induced Superconductivity in Strontium Titanate. *Phys. Rev. B: Condens. Matter Mater. Phys.* **2018**, *97* (14), 1−8.

(6) Miyata, K.; Zhu, X. Y. Riddles in Perovskite Research: Ferroelectric Large Polarons. *Nat. Mater.* **2018**, *17* (May), 379−381.

(7) Jiang, M. P.; Trigo, M.; Savic, I.; Fahy, S.; Murray, D.; Bray, C.; Clark, J.; Henighan, T.; Kozina, M.; Chollet, M.; Glownia, J. M.; Hoffmann, M. C.; Zhu, D.; Delaire, O.; May, A. F.; Sales, B. C.; Lindenberg, A. M.; Zalden, P.; Sato, T.; Merlin, R.; Reis, D. A. The Origin of Incipient Ferroelectricity in Lead Telluride. *Nat. Commun.* **2016**, *7*, 1−9.

(8) O'Hara, A.; Demkov, A. A. Nature of the Metal-Insulator Transition in $NbO_2$. *Phys. Rev. B: Condens. Matter Mater. Phys.* **2015**, *91* (9), 1−6.

(9) Wang, Z.; Rhodes, D. A.; Watanabe, K.; Taniguchi, T.; Hone, J. C.; Shan, J.; Mak, K. F. Evidence of High-Temperature Exciton Condensation in Two-Dimensional Atomic Double Layers. *Nature* **2019**, *574* (7776), 76−80.

(10) Kogar, A.; Rak, M. S.; Vig, S.; Husain, A. A.; Flicker, F.; Joe, Y.; Il; Venema, L.; MacDougall, G. J.; Chiang, T. C.; Fradkin, E.; Van Wezel, J.; Abbamonte, P. Signatures of Exciton Condensation in a Transition Metal Dichalcogenide. *Science* **2017**, *358* (6368), 1314−1317.

(11) Shuvaev, A. M.; Hemberger, J.; Niermann, D.; Schrettle, F.; Loidl, A.; Ivanov, V. Y.; Travkin, V. D.; Mukhin, A. A.; Pimenov, A. Soft-Mode Behavior of Electromagnons in Multiferroic Manganite. *Phys. Rev. B: Condens. Matter Mater. Phys.* **2010**, *82* (17), 1−5.

(12) Cowley, R. A. Soft Modes and Structural Phase Transitions. *Integr. Ferroelectr.* **2012**, *133* (1), 109−117.

(13) Fleury, P. A. The Effects of Soft Modes on the Structure and Properties of Materials. *Annu. Rev. Mater. Sci.* **1976**, *6* (1), 157−180.

(14) Gaillac, R.; Pullumbi, P.; Beyer, K. A.; Chapman, K.; Keen, D. A.; Bennett, T. D.; Coudert, F. X. Liquid Metal−Organic Frameworks. *Nat. Mater.* **2017**, *16* (11), 1149−1155.

(15) Costa Gomes, M.; Pison, L.; Červinka, C.; Padua, A. Porous Ionic Liquids or Liquid Metal-Organic Frameworks? *Angew. Chem., Int. Ed.* **2018**, 11909−11912.

(16) Longley, L.; Collins, S. M.; Li, S.; Smales, G. J.; Erucar, I.; Qiao, A.; Hou, J.; Doherty, C. M.; Thornton, A. W.; Hill, A. J.; Yu, X.; Terrill, N. J.; Smith, A. J.; Cohen, S. M.; Midgley, P. A.; Keen, D. A.; Telfer, S. G.; Bennett, T. D. Flux Melting of Metal-Organic Frameworks. *Chem. Sci.* **2019**, *10* (12), 3592−3601.

(17) Bumstead, A. M.; Ríos Gómez, M. L.; Thorne, M. F.; Sapnik, A. F.; Longley, L.; Tuffnell, J. M.; Keeble, D. S.; Keen, D. A.; Bennett, T. D. Investigating the Melting Behaviour of Polymorphic Zeolitic Imidazolate Frameworks. *CrystEngComm* **2020**, *22* (21), 3627−3637.

(18) Tuffnell, J. M.; Ashling, C. W.; Hou, J.; Li, S.; Longley, L.; Ríos Gómez, M. L.; Bennett, T. D. Novel Metal-Organic Framework Materials: Blends, Liquids, Glasses and Crystal-Glass Composites. *Chem. Commun.* **2019**, *55* (60), 8705−8715.

(19) Bennett, T. D.; Horike, S. Liquid, Glass and Amorphous Solid States of Coordination Polymers and Metal−Organic Frameworks. *Nat. Rev. Mater.* **2018**, *3* (11), 431−440.

(20) Ogawa, T.; Takahashi, K.; Nagarkar, S. S.; Ohara, K.; Hong, Y.; Nishiyama, Y.; Horike, S. Coordination Polymer Glass from a Protic Ionic Liquid: Proton Conductivity and Mechanical Properties as an Electrolyte. *Chem. Sci.* **2020**, *11* (20), 5175−5181.

(21) Horike, S.; Nagarkar, S. S.; Ogawa, T.; Kitagawa, S. A New Dimension for Coordination Polymers and Metal−Organic Frameworks: Towards Functional Glasses and Liquids. *Angew. Chem., Int. Ed.* **2020**, *59* (17), 6652−6664.

(22) Chen, W.; Horike, S.; Umeyama, D.; Ogiwara, N.; Itakura, T.; Tassel, C.; Goto, Y.; Kageyama, H.; Kitagawa, S. Glass Formation of a Coordination Polymer Crystal for Enhanced Proton Conductivity and Material Flexibility. *Angew. Chem., Int. Ed.* **2016**, *55* (17), 5195−5200.
(23) Zhou, C.; Longley, L.; Krajnc, A.; Smales, G. J.; Qiao, A.; Erucar, I.; Doherty, C. M.; Thornton, A. W.; Hill, A. J.; Ashling, C. W.; Qazvini, O. T.; Lee, S. J.; Chater, P. A.; Terrill, N. J.; Smith, A. J.; Yue, Y.; Mali, G.; Keen, D. A.; Telfer, S. G.; Bennett, T. D. Metal-Organic Framework Glasses with Permanent Accessible Porosity. *Nat. Commun.* **2018**, *9* (1), 1−9.
(24) Hou, J.; Ríos Gómez, M. L.; Krajnc, A.; McCaul, A.; Li, S.; Bumstead, A. M.; Sapnik, A. F.; Deng, Z.; Lin, R.; Chater, P. A.; Keeble, D. S.; Keen, D. A.; Appadoo, D.; Chan, B.; Chen, V.; Mali, G.; Bennett, T. D. Halogenated Metal-Organic Framework Glasses and Liquids. *J. Am. Chem. Soc.* **2020**, *142* (8), 3880−3890.
(25) Umeyama, D.; Funnell, N. P.; Cliffe, M. J.; Hill, J. A.; Goodwin, A. L.; Hijikata, Y.; Itakura, T.; Okubo, T.; Horike, S.; Kitagawa, S. Glass Formation via Structural Fragmentation of a 2D Coordination Network. *Chem. Commun.* **2015**, *51* (64), 12728−12731.
(26) Hou, J.; Ashling, C. W.; Collins, S. M.; Krajnc, A.; Zhou, C.; Longley, L.; Johnstone, D. N.; Chater, P. A.; Li, S.; Coulet, M. V.; Llewellyn, P. L.; Coudert, F. X.; Keen, D. A.; Midgley, P. A.; Mali, G.; Chen, V.; Bennett, T. D. Metal-Organic Framework Crystal-Glass Composites. *Nat. Commun.* **2019**, *10* (1), 1−10.
(27) Brozek, C. K.; Michaelis, V. K.; Ong, T.-C.; Bellarosa, L.; López, N.; Griffin, R. G.; Dincă, M. Dynamic DMF Binding in MOF-5 Enables the Formation of Metastable Cobalt-Substituted MOF-5 Analogues. *ACS Cent. Sci.* **2015**, *1* (5), 252−260.
(28) Krylov, A.; Vtyurin, A.; Petkov, P.; Senkovska, I.; Maliuta, M.; Bon, V.; Heine, T.; Kaskel, S.; Slyusareva, E. Raman Spectroscopy Studies of the Terahertz Vibrational Modes of a DUT-8 (Ni) Metal-Organic Framework. *Phys. Chem. Chem. Phys.* **2017**, *19* (47), 32099−32104.
(29) Hoffman, A. E. J.; Vanduyfhuys, L.; Nevjestić, I.; Wieme, J.; Rogge, S. M. J.; Depauw, H.; Van Der Voort, P.; Vrielinck, H.; Van Speybroeck, V. Elucidating the Vibrational Fingerprint of the Flexible Metal-Organic Framework MIL-53(Al) Using a Combined Experimental/Computational Approach. *J. Phys. Chem. C* **2018**, *122* (5), 2734−2746.
(30) Rao, Y. L.; Chortos, A.; Pfattner, R.; Lissel, F.; Chiu, Y. C.; Feig, V.; Xu, J.; Kurosawa, T.; Gu, X.; Wang, C.; He, M.; Chung, J. W.; Bao, Z. Stretchable Self-Healing Polymeric Dielectrics Cross-Linked through Metal-Ligand Coordination. *J. Am. Chem. Soc.* **2016**, *138* (18), 6020−6027.
(31) Williams, K. A.; Boydston, A. J.; Bielawski, C. W. Main-Chain Organometallic Polymers: Synthetic Strategies, Applications, and Perspectives. *Chem. Soc. Rev.* **2007**, *36* (5), 729.
(32) Norris, B. C.; Bielawski, C. W. Structurally Dynamic Materials Based on Bis(N-Heterocyclic Carbene)s and Bis(Isothiocyanate)s: Toward Reversible, Conjugated Polymers. *Macromolecules* **2010**, *43* (8), 3591−3593.
(33) Williams, K. A.; Dreyer, D. R.; Bielawski, C. W. The Underlying Chemistry of Self-Healing Materials. *MRS Bull.* **2008**, *33* (08), 759−765.
(34) Winter, A.; Schubert, U. S. Synthesis and Characterization of Metallo-Supramolecular Polymers. *Chem. Soc. Rev.* **2016**, *45* (19), 5311−5357.
(35) Dobrawa, R.; Würthner, F. Metallosupramolecular Approach toward Functional Coordination Polymers. *J. Polym. Sci., Part A: Polym. Chem.* **2005**, *43* (21), 4981−4995.
(36) Lewis, A. K. de K.; Caddick, S.; Cloke, F. G. N.; Billingham, N. C.; Hitchcock, P. B.; Leonard, J. Synthetic, Structural, and Mechanistic Studies on the Oxidative Addition of Aromatic Chlorides to a Palladium (N-Heterocyclic Carbene) Complex: Relevance to Catalytic Amination. *J. Am. Chem. Soc.* **2003**, *125* (33), 10066−10073.
(37) Bunting, J. W.; Thong, K. M. Stability Constants for Some 1:1 Metal−Carboxylate Complexes. *Can. J. Chem.* **1970**, *48* (11), 1654−1656.
(38) Grosch, J. S.; Paesani, F. Molecular-Level Characterization of the Breathing Behavior of the Jungle-Gym-Type DMOF-1 Metal-Organic Framework. *J. Am. Chem. Soc.* **2012**, *134* (9), 4207−4215.
(39) Yot, P. G.; Ma, Q.; Haines, J.; Yang, Q.; Ghoufi, A.; Devic, T.; Serre, C.; Dmitriev, V.; Férey, G.; Zhong, C.; Maurin, G. Large Breathing of the MOF MIL-47($V^{IV}$) under Mechanical Pressure: A Joint Experimental-Modelling Exploration. *Chem. Sci.* **2012**, *3* (4), 1100−1104.
(40) Ghoufi, A.; Benhamed, K.; Boukli-Hacene, L.; Maurin, G. Electrically Induced Breathing of the MIL-53(Cr) Metal-Organic Framework. *ACS Cent. Sci.* **2017**, *3* (5), 394−398.
(41) Parent, L. R.; Pham, C. H.; Patterson, J. P.; Denny, M. S.; Cohen, S. M.; Gianneschi, N. C.; Paesani, F. Pore Breathing of Metal−Organic Frameworks by Environmental Transmission Electron Microscopy. *J. Am. Chem. Soc.* **2017**, *139* (40), 13973−13976.
(42) Nishida, J.; Tamimi, A.; Fei, H.; Pullen, S.; Ott, S.; Cohen, S. M.; Fayer, M. D. Structural Dynamics inside a Functionalized Metal-Organic Framework Probed by Ultrafast 2D IR Spectroscopy. *Proc. Natl. Acad. Sci. U. S. A.* **2014**, *111* (52), 18442−18447.
(43) Mao, V. Y.; Milner, P. J.; Lee, J.-H.; Forse, A. C.; Kim, E. J.; Siegelman, R. L.; McGuirk, C. M.; Porter-Zasada, L. B.; Neaton, J. B.; Reimer, J. A.; Long, J. R. Cooperative Carbon Dioxide Adsorption in Alcoholamine- and Alkoxyalkylamine-Functionalized Metal-Organic Frameworks. *Angew. Chem., Int. Ed.* **2020**, *59*, 19468.
(44) McDonald, T. M.; Mason, J. A.; Kong, X.; Bloch, E. D.; Gygi, D.; Dani, A.; Crocellà, V.; Giordanino, F.; Odoh, S. O.; Drisdell, W. S.; Vlaisavljevich, B.; Dzubak, A. L.; Poloni, R.; Schnell, S. K.; Planas, N.; Lee, K.; Pascal, T.; Wan, L. F.; Prendergast, D.; Neaton, J. B.; Smit, B.; Kortright, J. B.; Gagliardi, L.; Bordiga, S.; Reimer, J. A.; Long, J. R. Cooperative Insertion of $CO_2$ in Diamine-Appended Metal-Organic Frameworks. *Nature* **2015**, *519* (7543), 303−308.
(45) Kong, X.; Scott, E.; Ding, W.; Mason, J. A.; Long, J. R.; Reimer, J. A. $CO_2$ Dynamics in a Metal-Organic Framework with Open Metal Sites. *J. Am. Chem. Soc.* **2012**, *134* (35), 14341−14344.
(46) Brozek, C. K.; Ozarowski, A.; Stoian, S. A.; Dincă, M. Dynamic Structural Flexibility of Fe-MOF-5 Evidenced by $^{57}$Fe Mössbauer Spectroscopy. *Inorg. Chem. Front.* **2017**, *4* (5), 782−788.
(47) Wu, Y.; Kobayashi, A.; Halder, G. J.; Peterson, V. K.; Chapman, K. W.; Lock, N.; Southon, P. D.; Kepert, C. J. Negative Thermal Expansion in the Metal-Organic Framework Material $Cu_3$(1,3,5-Benzenetricarboxylate)$_2$. *Angew. Chem., Int. Ed.* **2008**, *47* (46), 8929−8932.
(48) Lock, N.; Christensen, M.; Kepert, C. J.; Iversen, B. B. Effect of Gas Pressure on Negative Thermal Expansion in MOF-5. *Chem. Commun.* **2013**, *49* (8), 789−791.
(49) Zhou, W.; Wu, H.; Yildirim, T.; Simpson, J. R.; Walker, A. R. H. Origin of the Exceptional Negative Thermal Expansion in Metal-Organic Framework-5 $Zn_4O$(1,4-Benzenedicarboxylate)$_3$. *Phys. Rev. B: Condens. Matter Mater. Phys.* **2008**, *78* (5), 1−5.
(50) Schneider, C.; Bodesheim, D.; Ehrenreich, M. G.; Crocella, V.; Mink, J.; Fischer, R. A.; Butler, K. T.; Kieslich, G. Tuning the Negative Thermal Expansion Behavior of the Metal−Organic Framework $Cu_3BTC_2$ by Retrofitting. *J. Am. Chem. Soc.* **2019**, *141* (26), 10504−10509.
(51) Redfern, L. R.; Ducamp, M.; Wasson, M. C.; Robison, L.; Son, F. A.; Coudert, F.-X.; Farha, O. K. Isolating the Role of the Node-Linker Bond in the Compression of UiO-66 Metal−Organic Frameworks. *Chem. Mater.* **2020**, *32* (13), 5864−5871.
(52) Lock, N.; Christensen, M.; Wu, Y.; Peterson, V. K.; Thomsen, M. K.; Piltz, R. O.; Ramirez-Cuesta, A. J.; McIntyre, G. J.; Norén, K.; Kutteh, R.; Kepert, C. J.; Kearley, G. J.; Iversen, B. B. Scrutinizing Negative Thermal Expansion in MOF-5 by Scattering Techniques and Ab Initio Calculations. *Dalt. Trans.* **2013**, *42* (6), 1996−2007.
(53) Lock, N.; Wu, Y.; Christensen, M.; Cameron, L. J.; Peterson, V. K.; Bridgeman, A. J.; Kepert, C. J.; Iversen, B. B. Elucidating Negative Thermal Expansion in MOF-5. *J. Phys. Chem. C* **2010**, *114* (39), 16181−16186.


https://dx.doi.org/10.1021/jacs.0c09499
J. Am. Chem. Soc. 2020, 142, 19291−19299

(54) Brozek, C. K.; Dinca, M. Cation Exchange at the Secondary Building Units of Metal-Organic Frameworks. *Chem. Soc. Rev.* **2014**, *43* (16), 5456−5467.
(55) Brozek, C. K.; Dincă, M. Lattice-Imposed Geometry in Metal−Organic Frameworks: Lacunary $Zn_4O$ Clusters in MOF-5 Serve as Tripodal Chelating Ligands for $Ni^{2+}$. *Chem. Sci.* **2012**, *3* (6), 2110.
(56) Brozek, C. K.; Bellarosa, L.; Soejima, T.; Clark, T. V.; Lõpez, N.; Dinca, M. Solvent-Dependent Cation Exchange in Metal-Organic Frameworks. *Chem. - Eur. J.* **2014**, *20*, 6871.
(57) Brozek, C. K.; Dinca, M. Thermodynamic Parameters of Cation Exchange in MOF-5 and MFU-4l. *Chem. Commun.* **2015**, *51* (59), 11780−11782.
(58) Takaishi, S.; DeMarco, E. J.; Pellin, M. J.; Farha, O. K.; Hupp, J. T. Solvent-Assisted Linker Exchange (SALE) and Post-Assembly Metallation in Porphyrinic Metal−Organic Framework Materials. *Chem. Sci.* **2013**, *4* (4), 1509.
(59) Kim, M.; Cahill, J. F.; Su, Y.; Prather, K. A.; Cohen, S. M. Postsynthetic Ligand Exchange as a Route to Functionalization of "inert" Metal-Organic Frameworks. *Chem. Sci.* **2012**, *3* (1), 126−130.
(60) Cohen, S. M. The Postsynthetic Renaissance in Porous Solids. *J. Am. Chem. Soc.* **2017**, *139* (8), 2855−2863.
(61) Leus, K.; Muylaert, I.; Vandichel, M.; Marin, G. B.; Waroquier, M.; Van Speybroeck, V.; Van der Voort, P. The Remarkable Catalytic Activity of the Saturated Metal Organic Framework V-MIL-47 in the Cyclohexene Oxidation. *Chem. Commun.* **2010**, *46* (28), 5085.
(62) Bode, S.; Zedler, L.; Schacher, F. H.; Dietzek, B.; Schmitt, M.; Popp, J.; Hager, M. D.; Schubert, U. S. Self-Healing Polymer Coatings Based on Crosslinked Metallosupramolecular Copolymers. *Adv. Mater.* **2013**, *25* (11), 1634−1638.
(63) Shen, Y. C.; Upadhya, P. C.; Linfield, E. H.; Davies, A. G. Temperature-Dependent Low-Frequency Vibrational Spectra of Purine and Adenine. *Appl. Phys. Lett.* **2003**, *82* (14), 2350−2352.
(64) Chakravarty, C.; Debenedetti, P. G.; Stillinger, F. H. Lindemann Measures for the Solid-Liquid Phase Transition. *J. Chem. Phys.* **2007**, *126* (20), 204508.
(65) Leong, W. L.; Vittal, J. J. One-Dimensional Coordination Polymers: Complexity and Diversity in Structures, Properties, and Applications. *Chem. Rev.* **2011**, *111* (2), 688−764.
(66) Gosselin, E. J.; Rowland, C. A.; Bloch, E. D. Permanently Microporous Metal−Organic Polyhedra. *Chem. Rev.* **2020**, *120* (16), 8987−9014.
(67) Cooper, A. I. Porous Molecular Solids and Liquids. *ACS Cent. Sci.* **2017**, *3* (6), 544−553.
(68) Tiana, D.; Hendon, C. H.; Walsh, A. Ligand Design for Long-Range Magnetic Order in Metal-Organic Frameworks. *Chem. Commun.* **2014**, *50* (90), 13990−13993.
(69) Xu, B.; Poduska, K. M. Linking Crystal Structure with Temperature-Sensitive Vibrational Modes in Calcium Carbonate Minerals. *Phys. Chem. Chem. Phys.* **2014**, *16* (33), 17634−17639.
(70) Balan, E.; Delattre, S.; Roche, D.; Segalen, L.; Morin, G.; Guillaumet, M.; Blanchard, M.; Lazzeri, M.; Brouder, C.; Salje, E. K. H. Line-Broadening Effects in the Powder Infrared Spectrum of Apatite. *Phys. Chem. Miner.* **2011**, *38* (2), 111−122.
(71) Bien, C. E.; Chen, K. K.; Chien, S.-C.; Reiner, B. R.; Lin, L.-C.; Wade, C. R.; Ho, W. S. W. Bioinspired Metal−Organic Framework for Trace $CO_2$ Capture. *J. Am. Chem. Soc.* **2018**, *140* (40), 12662−12666.
(72) Huang, C. Y.; Wang, T.; Gai, F. Temperature Dependence of the CN Stretching Vibration of a Nitrile-Derivatized Phenylalanine in Water. *Chem. Phys. Lett.* **2003**, *371* (5−6), 731−738.
(73) Lee, S.; Bürgi, H.-B.; Alshmimri, S. A.; Yaghi, O. M. Impact of Disordered Guest−Framework Interactions on the Crystallography of Metal−Organic Frameworks. *J. Am. Chem. Soc.* **2018**, *140* (28), 8958−8964.
(74) Rodríguez-Velamazán, J. A.; González, M. A.; Real, J. A.; Castro, M.; Muñoz, M. C.; Gaspar, A. B.; Ohtani, R.; Ohba, M.; Yoneda, K.; Hijikata, Y.; Yanai, N.; Mizuno, M.; Ando, H.; Kitagawa, S. A Switchable Molecular Rotator: Neutron Spectroscopy Study on a Polymeric Spin-Crossover Compound. *J. Am. Chem. Soc.* **2012**, *134* (11), 5083−5089.
(75) Sirenko, A. A.; Clark, A. M.; Hao, J.; Si, W.; Xi, X. X. Soft-Mode Hardening in $SrTiO_3$ Thin Films. *Nature* **2000**, *9*, 373−376.
(76) Zhou, J. J.; Hellman, O.; Bernardi, M. Electron-Phonon Scattering in the Presence of Soft Modes and Electron Mobility in $SrTiO_3$ Perovskite from First Principles. *Phys. Rev. Lett.* **2018**, *121* (22), 226603.
(77) Hoffman, A. E. J.; Wieme, J.; Rogge, S. M. J.; Vanduyfhuys, L.; Van Speybroeck, V. The Impact of Lattice Vibrations on the Macroscopic Breathing Behavior of MIL-53(Al). *Z. Kristallogr. - Cryst. Mater.* **2019**, *234* (7−8), 529−545.
(78) Liu, L.; Li, L.; Ziebel, M. E.; Harris, T. D. Metal-Diamidobenzoquinone Frameworks via Post-Synthetic Linker Exchange. *J. Am. Chem. Soc.* **2020**, *142* (10), 4705−4713.
(79) Morabito, J. V.; Chou, L. Y.; Li, Z.; Manna, C. M.; Petroff, C. A.; Kyada, R. J.; Palomba, J. M.; Byers, J. A.; Tsung, C. K. Molecular Encapsulation beyond the Aperture Size Limit through Dissociative Linker Exchange in Metal-Organic Framework Crystals. *J. Am. Chem. Soc.* **2014**, *136* (36), 12540−12543.
(80) Balestra, S. R. G.; Bueno-Perez, R.; Hamad, S.; Dubbeldam, D.; Ruiz-Salvador, A. R.; Calero, S. Controlling Thermal Expansion: A Metal-Organic Frameworks Route. *Chem. Mater.* **2016**, *28* (22), 8296−8304.
(81) Rimmer, L. H. N.; Dove, M. T.; Goodwin, A. L.; Palmer, D. C. Acoustic Phonons and Negative Thermal Expansion in MOF-5. *Phys. Chem. Chem. Phys.* **2014**, *16* (39), 21144−21152.


https://dx.doi.org/10.1021/jacs.0c09499
J. Am. Chem. Soc. 2020, 142, 19291−19299